Cancer Cell
Article

Targeted Inactivation of *Fh1* Causes Proliferative Renal Cyst Development and Activation of the Hypoxia Pathway

Patrick J. Pollard,[1,*] Bradley Spencer-Dene,[2,7] Deepa Shukla,[8] Kimberley Howarth,[1] Emma Nye,[2,7] Mona El-Bahrawy,[7] Maesha Deheragoda,[4] Maria Joannou,[2,7] Stuart McDonald,[4] Alison Martin,[6] Peter Igarashi,[9] Sunita Varsani-Brown,[5] Ian Rosewell,[5] Richard Poulsom,[3] Patrick Maxwell,[8] Gordon W. Stamp,[2,7] and Ian P.M. Tomlinson[1,10]

[1] Molecular and Population Genetics Laboratory
[2] Experimental Pathology Laboratory
[3] In Situ Hybridisation Service
[4] Histopathology Department
[5] Transgenic Services
[6] Biological Resources
London Research Institute, Cancer Research UK, 44, Lincoln's Inn Fields, London WC2A 3PX, United Kingdom
[7] Department of Histopathology
[8] Division of Renal Medicine
Hammersmith Hospital, Imperial College London, Du Cane Road, London, W12 0NN, United Kingdom
[9] Division of Nephrology, University of Texas Southwestern Medical Center, 5323 Harry Hines Boulevard, Dallas, TX 75390-8856, USA
[10] Barts and the London Medical School, Queen Mary College, London, E1 2AD, United Kingdom
*Correspondence: patrick.pollard@cancer.org.uk
DOI 10.1016/j.ccr.2007.02.005

SUMMARY

Germline mutations in the fumarate hydratase (*FH*) tumor suppressor gene predispose to leiomyomatosis, renal cysts, and renal cell cancer (HLRCC). HLRCC tumors overexpress HIF1α and hypoxia pathway genes. We conditionally inactivated mouse *Fh1* in the kidney. *Fh1* mutants developed multiple clonal renal cysts that overexpressed Hif1α and Hif2α. Hif targets, such as *Glut1* and *Vegf*, were upregulated. We found that Fh1-deficient murine embryonic stem cells and renal carcinomas from HLRCC showed similar overexpression of HIF and hypoxia pathway components to the mouse cysts. Our data have shown in vivo that pseudohypoxic drive, resulting from HIF1α (and HIF2α) overexpression, is a direct consequence of Fh1 inactivation. Our mouse may be useful for testing therapeutic interventions that target angiogenesis and HIF-prolyl hydroxylation.

INTRODUCTION

The *FH* tumor suppressor gene encodes the Krebs cycle enzyme fumarate hydratase and is mutated in individuals with the Mendelian syndrome of hereditary leiomyomatosis and renal cell cancer (HLRCC) (Tomlinson et al., 2002; Toro et al., 2003). Individuals with HLRCC develop benign smooth-muscle neoplasms of the skin and uterus and may develop solitary renal cell cancers, of type II papillary or collecting-duct morphology (Alam et al., 2003; Kiuru and Launonen, 2004; Kiuru et al., 2001; Tomlinson et al., 2002; Toro et al., 2003). A few HLRCC patients may also develop leiomyosarcomas and many develop benign renal cysts (Lehtonen et al., 2005). Most HLRCC tumors

SIGNIFICANCE

HIF overexpression occurs (1) in renal cancers from the familial cancer syndrome HLRCC, which results from germline mutations in the Krebs cycle gene fumarate hydratase (*FH*), and (2) in cancers from von Hippel-Lindau disease patients. In vitro inactivation of *FH* leads to HIF1α overexpression. Here, we directly link kidney-specific, biallelic inactivation of murine *Fh1* to pseudohypoxic drive in vivo. Like humans with HLRCC, $Fh1^{-/-}$ animals develop renal cysts. These cysts are clonal and proliferative, and they show overexpression of HIF and hypoxia pathway components. This overexpression is also seen in $Fh1^{-/-}$ ES cells. Our mouse model advances the understanding of biochemical pathways linking mitochondrial dysfunction and tumorigenesis and will allow testing of potential therapies for renal neoplasms.

exhibit activation of the hypoxia pathway: they overexpress hypoxia-inducible factor-1-α (HIF1α) and its target genes, such as vascular endothelial growth factor (*VEGF*) and *BNIP3*, and have increased vascularity in comparison to their sporadic counterparts (Pollard et al., 2005a, 2005b). This evidence suggests that "pseudohypoxic drive"—that is, constitutive expression of HIF1α in normoxia—plays a significant role in the pathogenesis of HLRCC neoplasms. Indeed, pseudohypoxia is evident in the pathogenesis of other familial cancers such as those in von Hippel-Lindau (VHL) disease (Iliopoulos and Kaelin, 1997; Maher and Kaelin, 1997) and hereditary paraganglioma tosis (HPGL) (Gimenez-Roqueplo et al., 2001, 2002; Pollard et al., 2005b), the latter arising in patients with germline succinate dehydrogenase (*SDHB/C/D*) mutations (Baysal et al., 2002).

HIF is a transcription factor that is activated in all cells when oxygen tension is low, and VHL acts as the recognition component of an ubiquitin E3 ligase complex that inactivates HIF in the presence of oxygen (Ivan et al., 2001; Jaakkola et al., 2001; Lisztwan et al., 1999; Maxwell et al., 1999). HIF was originally identified from studies of the erythropoietin gene but is now recognized to regulate a very wide range of other genes, including those encoding proteins involved in glucose metabolism and angiogenesis (Carmeliet et al., 1998; Pugh and Ratcliffe, 2003). A HIF complex consists of a regulatory α subunit and a constitutively expressed β subunit (Wang et al., 1995). Under well-oxygenated conditions, VHL acts as a recognition molecule that targets HIFα subunits for proteosomal degradation. Two specific proline residues in the oxygen-dependent degradation domain (ODDD) of HIF1α and an asparagine in the transactivation domain are respectively hydroxylated by the dioxygenases PHD1-3 and FIH (Ivan et al., 2001; Jaakkola et al., 2001; Masson and Ratcliffe, 2003; Schofield and Ratcliffe, 2004). Prolyl hydroxylation within the ODDD allows VHL to interact with the HIFα subunit, leading to its ubiquitylation and destruction. Asparaginyl hydroxylation prevents transactivator recruitment, thus inactivating HIF through a second route (Masson and Ratcliffe, 2003). When the level of oxygen is low, HIFα subunits are protected from hydroxylation, dimerize with a β subunit to form a HIF complex and interact with hypoxic response elements in promoter/enhancer regions, and recruit coactivators to modulate the expression of a large number of genes (Carmeliet et al., 1998; Talks et al., 2000)

We have shown that HLRCC tumors accumulate fumarate and succinate in vivo (Pollard et al., 2005b). In vitro studies have demonstrated that siRNA knockdown (and biochemical inhibition) of *FH* and *SDH* can cause failure of the PHDs to hydroxylate HIF1α (Isaacs et al., 2005; Selak et al., 2005) because this reaction relies on conversion of α-ketoglutarate to succinate. Such in vitro studies inevitably have well-characterized limitations, such as the inability to study the tissue environment or the cell of origin of the human tumors and the abnormal (epi)genetic complement of most cultured cells, especially if derived from tumors. Moreover, there is no commercially available specific pharmacological inhibitor of FH, forcing reliance on 3-nitropropionic acid (3-NPA), a molecule that also inhibits SDH (Binienda et al., 2001; Selak et al., 2005; Zeevalk et al., 1995).

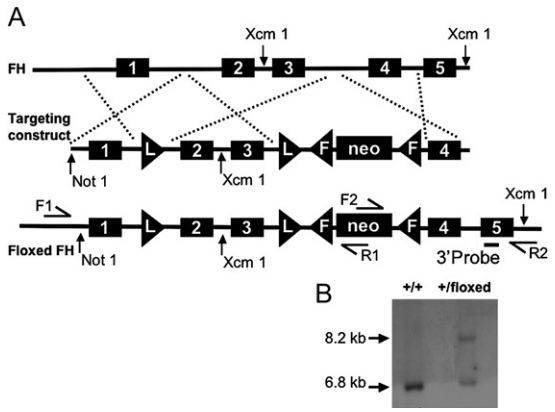

Figure 1. Targeting Strategy for the Fh1 Conditional Knockout Mouse

We used homologous recombination to replace the wild-type allele with the targeted allele, flanking exons 2 and 3 of *Fh1* by loxP sites to allow conditional gene inactivation. Comparison with human HLRCC *FH* mutations shows that deletion of these exons would cause loss of protein function. The targeting construct (A) contained the prokaryotic neomycin resistance gene (*neo*) flanked by Frt sites (F) and three arms of genomic DNA homologous to the *Fh1* locus. LoxP sites (L) flanked the 3.0 kb middle arm. This targeting construct was transferred into ES cells by electroporation, and cells were selected for G418S resistance. ES cell clones were isolated and analyzed initially by PCR for 3′ and 5′ site-specific integration into the *Fh1* locus. Further analysis of positive clones by Southern blotting confirmed the proper integration of the targeted allele (B). Two independent clones were used for blastocyst injection to generate chimeras from which we obtained heterozygous F1 offspring, which were also identified by PCR and Southern blotting (data not shown). The neomycin cassette, flanked by Frt sites, was excised in vivo by crossing with mice expressing enhanced Flp recombinase under the ubiquitous phosphoglycerate kinase (*Pgk*) promoter.

In order to provide a model of HLRCC, and potentially a more general model of Krebs cycle dysfunction in tumorigenesis, we constructed an *Fh1* "knockout" mouse.

RESULTS

We created a conditionally targeted *Fh1* mutant allele ($Fh1^{fl}$), thus facilitating tissue-specific and/or temporal biallelic *Fh1* inactivation (Figure 1) and analysis of the downstream functional consequences. $Fh1^{-/-}$ mice died in early embryogenesis (Figure 2). In order to study specific inactivation of *Fh1* in the kidney, $Fh1^{fl/+}$ mice were bred with mice expressing Cre recombinase under the Ksp-Cadherin promoter (Ksp1.3/Cre) (Shao et al., 2002a, 2002b). The $Fh1^{fl/+}$ Ksp1.3/Cre mice were then intercrossed to produce homozygous conditional knockout $Fh1^{fl/fl}$ Ksp1.3/Cre progeny.

$Fh1^{fl/fl}$ Ksp1.3/Cre animals appeared healthy until 8 months of age, when polyuric renal failure became apparent in some animals (data not shown). All other animals of

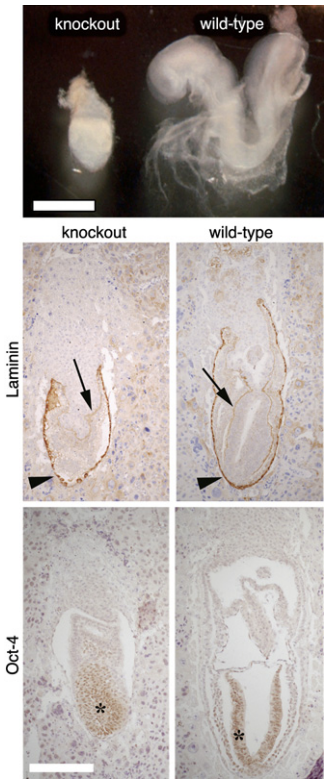

Figure 2. Fh1 Null Mice Die during Early Embryogenesis

Fh1$^{fl/+}$ mice were bred with *Pgk*-Cre$^{+/-}$ mice to generate heterozygous *Fh1*$^{+/-}$ knockout mice. To obtain *Fh1*$^{-/-}$ embryos, *Fh1*$^{+/-}$ heterozygous mice were crossed. Litters were examined over a range of gestational stages with the morning of finding the plug determined as embryonic day (E) 0.5. In order to discriminate between the wild-type and the mutant alleles, the three-primer PCR analysis was used (see Experimental Procedures) using yolk sac DNA. We genotyped 176 animals born from matings between heterozygous *Fh1*$^{+/-}$ parents, of which 59 (33%) were *Fh1*$^{+/+}$ and 117 (66%) were *Fh1*$^{+/-}$, with no *Fh1*$^{-/-}$ animals detected. Analysis of *Fh1*$^{-/-}$ embryos indicated lethality at E6.0. At E8.0, *Fh1*$^{-/-}$ (knockout) embryos had failed to develop beyond the egg-cylinder stage and were subsequently resorbed in utero (top; scale bar, 0.5 mm). Embryos at E7.0 were formalin fixed, paraffin embedded, and analyzed immunohistochemically (middle and lower; scale bar, 200 μm for all panels) for expression of laminin and Oct-4. Wild-type (right) and mutant (left) embryos expressed both proteins. Laminin was detected in the embryonic basement membrane (arrow) and in Reichert's membrane (parietal endoderm) (arrowhead). Oct-4 was expressed in the primitive embryonic ectoderm (asterisk).

this genotype (n = 26) eventually became ill, the oldest presenting at 15 months of age. Postmortem examination showed macroscopic renal cysts in all *Fh1*$^{fl/fl}$ Ksp1.3/Cre animals (Figure 3). The kidneys showed extensive cystic change in the cortico-medullary junction with irregular cysts lined by cuboidal epithelium, consistent with a derivation from the loop of Henle. There was, in addition, mild hydronephrosis in animals more than 14 months old. The proximal and distal convoluted tubules appeared grossly normal, although occasional glomeruli were sclerosed. Focal minor inflammatory infiltrate was minimal. Some of the tubules were lined by vacuolated epithelium containing proteinaceous debris, but most contained small amounts of pale eosinophilic secretion, and some of the cells lining these cysts appeared to show poor intercellular cohesion and mild nuclear variation.

PAS staining (data not shown) revealed the cyst-lining epithelium to be negative, in contrast to the convoluted tubular epithelium, indicating that the cysts were derived from the loop of Henle. The cytoplasm of the epithelial cells lining the cysts stained negatively for aquaporin1, positively for aquaporin2 (53.3%), and positively for Tamm-Horsfall protein (Thp) (57.0%), showing that the majority of cysts were derived from the collecting ducts and the thick ascending limb of the loop of Henle (Figure 3). Kidneys from asymptomatic *Fh1*$^{fl/fl}$ Ksp1.3/Cre animals aged less than 10 months revealed similar cysts and some mild pelvic dilatation. Sections taken through the ureters appeared normal, and no organic blockage was evident at the pelvi-ureteric junction. The medulla of the kidneys was normal. Although most mice of all genotypes developed microscopic (<0.5 mm diameter), age-related renal cysts, no abnormal renal or other phenotype (Figure 3) was found in the control littermates (*Cre*$^{-/-}$ and/or *Fh1*$^{+/+}$ animals) or in the mutant heterozygotes (*Fh1*$^{fl/+}$; Ksp1.3-Cre$^{+/-}$).

In order to confirm *Cre*-mediated *Fh1* deletion in the renal cysts, we used in situ hybridization (ISH) to show absence of *Fh1* mRNA specifically in the cells lining the cysts (Figure 4). Additionally, five cysts were isolated using laser-capture microdissection and PCR genotyped for the targeted and deleted *Fh1* allele. All cysts showed absence of the targeted allele and the presence of the recombined (deleted) allele (1 flox) (Figure 4). By comparison, adjacent renal cortex showed the presence of the targeted (functional) *Fh1* allele (termed 2 flox); in some cases, the deleted allele was also present (Figure 4), showing that Cre-mediated recombination of at least one allele had occurred in some morphologically normal cells, and that "two hits" were necessary for cyst formation.

In order to test whether the cysts were derived from the proliferation of a single cell, we used enzyme histochemistry to search for loss of mitochondrial cytochrome *c* oxidase, a rare phenomenon that occurs spontaneously with age. This method has been used previously to demonstrate clonal origins in the gastrointestinal tract (Greaves et al., 2006). No loss of cytochrome *c* oxidase activity was observed in kidneys from wild-type mice or in noncystic tissue from knockout animals, showing polyclonal origins. However, occasional absence of activity was found in cysts from knockout animals (Figure 5). Smaller cysts showed uniform loss of activity in the cyst epithelium, demonstrating monoclonal origin. Some larger cysts showed patches of absent activity, together with patches of normal activity. Given that cytochrome *c* oxidase inactivation is a very rare event (<1 in 200 cysts), by far the most probable explanation for the "mixed" larger cysts was fusion between smaller cysts.

Renal cysts from ten animals (five knockouts and five *Fh1* wild-type littermate controls) were analyzed for

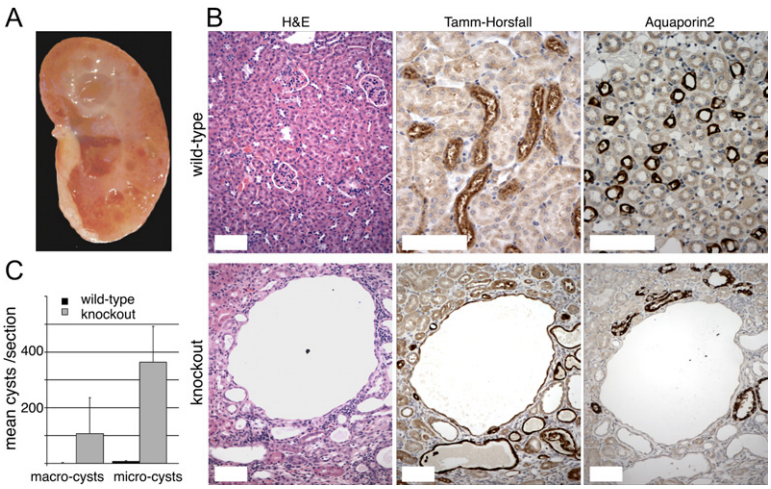

Figure 3. Mice with Renal-Specific Fh1 Knockout Develop Multiple Tubule-Derived Cysts

(A) The figure shows gross features of a bisected kidney from an *Fh1*$^{fl/fl}$ Ksp1.3/Cre mouse aged 12 months.

(B) The figure (scale bars, 250 μm) shows H&E staining of typical wild-type and cystic *Fh1* knockout kidneys. Thp immunostaining of wild-type and knockout kidneys indicates origin of this cyst from the thick ascending limb of the loop of Henle. Aquaporin2 immunostaining of wild-type and knockout kidneys indicates that the cyst is not collecting-duct derived.

(C) A cut-off of >0.1 mm diameter was used to classify a lesion as a cyst, and >0.5 mm diameter was used to classify a cyst as macroscopic. The median numbers of macroscopic and microscopic cysts detected in hemisections of kidneys of eight knockout (*Fh1*$^{fl/fl}$ Ksp1.3/Cre) and eight control mice are shown (for the microscopic cysts, p = 0.0006; for the macroscopic cysts, p = 0.0008, Mann-Whitney test). Kidney size did not differ significantly between the two groups of mice (details not shown). y error bars indicate ±SEM.

expression of Hif1α, Hif2α, glucose transporter 1 (Glut1), and carbonic anhydrase IX (Caix) proteins and separately assessed using ISH for *Vegf* and transforming growth factor α (*Tgfa*) mRNA expression. Hif1α was overexpressed (mean = 53% positive cyst nuclei, median = 50%, IQR = 48%–57% [Figures 6 and 7]) in the epithelia of all renal cysts from knockout animals, compared with noncystic kidney from the same animals, in which only occasional expression (<1% of nuclei) was found (Figure 6). Nuclear Hif2α overexpression (Figure 6) was also found consistently in cysts from the knockouts, although in a lower proportion of cyst epithelial cells (mean = 27% positive cyst nuclei, median = 24%, IQR = 21%–31%) than Hif1α (Figure 6); again only occasional Hif2α expression was found in the noncystic kidney. There was no association (positive or negative) between Hif1α and Hif2α expression (details not shown). Glut1 and *Vegf* overexpression were found wherever there was Hif1α overexpression (Figure 6), consistent with previous reports of these being Hif1α targets (Boado and Pardridge, 2002; Levy et al., 1996). Interestingly, however, expression of the HIF1α target Caix was almost undetectable in the cysts. Moreover, the Hif2α-target *Tgfa* was not expressed in any cyst, even those with positive Hif2α staining. In the microcysts from the control animals, few nuclei (<5%) showed nuclear expression of Hif1α, Hif2α, or their targets (Figure 6); noncystic renal tissue from the controls showed very occasional expression (<1% of nuclei) of either protein. Although the TUNEL assay showed no difference between the knockout cysts and wild-type microcysts as regards apoptotic cells, the knockout cysts did show evidence of greater proliferation (p = 0.0009, Mann-Whitney test), since Ki67 staining was more frequent (median = 7.5% cells) compared with the wild-type (median = 2.0% of cells) (Figure 6).

In order to corroborate our in vivo data, we inactivated *Fh1* by expression of Cre recombinase in *Fh1*$^{fl/-}$ embryonic stem (ES) cells from our mice. Replicate experiments showed that, after 48 hr, the Cre-transfected cells, but not controls, had greatly decreased expression of Fh1 that was accompanied by increased levels of Hif1α (Figure 7).

So as to provide evidence for a common pathway of pathogenesis in *Fh1*$^{-/-}$ murine cysts and human tumors with biallelic *FH* mutations, we analyzed five HLRCC type II papillary RCCs (Alam et al., 2005; Kiuru et al., 2001; Tomlinson et al., 2002) for expression of both HIFα isoforms and the target gene products GLUT1 and CAIX. As in the murine renal cysts, both HIF1α and HIF2α were overexpressed, with the latter again seen in fewer nuclei (median = 24% cancer nuclei positive for HIF1α, IQR = 19%–34%; median = 9% nuclei positive for HIF2α, IQR = 6%–11%). GLUT1 protein was highly expressed when HIF1α was overexpressed (Figure 6). Similarly to the cysts, CAIX expression was minimal.

DISCUSSION

Our in vivo model has shown that *Fh1* inactivation in the kidney causes the development of abnormally large and numerous cysts that have monoclonal origins and, even at the earliest stages, have acquired activation of the hypoxia pathway. Both HIF1α and HIF2α expression are found in these cysts, although the former predominates. It seems most plausible that activation of the hypoxia pathway is the cause of the cysts, probably through moderately increased cell proliferation. It is notable that inactivation of *Vhl* in the mouse kidney using a different mechanism of *Cre* expression also causes cystic disease, albeit in a minority of animals (Rankin et al., 2006). Moreover, both VHL and HLRCC patients develop multiple renal cysts, and these are likely to be premalignant lesions (Mandriota et al., 2002); it is entirely possible that if the cysts of our mice had not caused renal failure, progression to dysplasia and subsequent malignancy would have occurred. Pseudohypoxic drive is widely considered to contribute, at least in part, to tumorigenesis in VHL disease, HLRCC, HPGL, and many sporadic cancers. Although assay of PHD activity was

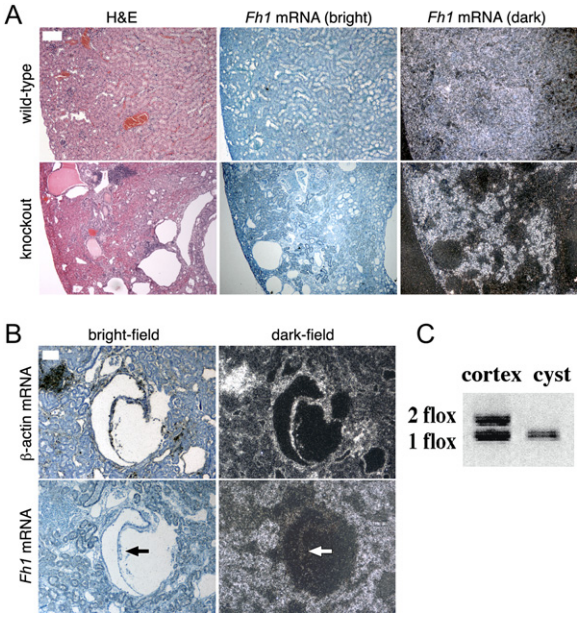

Figure 4. Comparison of Representative Serial Sections Shows Homozygous Knockout of Fh1 in Epithelial Lining of Renal Cysts

(A) Control (*Fh1*$^{fl/fl}$; Ksp1.3-Cre$^{-/-}$) and knockout mice (*Fh1*$^{fl/fl}$; Ksp1.3-Cre$^{+/-}$) stained with H&E and analyzed for expression of *Fh1* mRNA. Note absence of *Fh1* expression in the knockout cystic epithelium (β-actin-positive control not shown). Scale bar, 500 μm for each panel.

(B) Sections of a complex cyst in a knockout animal: expression of β-actin mRNA is present in the cyst epithelium, but *Fh1* mRNA expression is absent as indicated by the arrow. Scale bar, 250 μm for each panel.

(C) Results of laser-capture dissection and genomic PCR analysis of this cyst, with one band (1 flox) indicating the presence of one loxP site and homozygous deletion of *Fh1*; this is compared with the two bands in the renal cortex (2 flox, indicating the presence of two loxP sites, and 1 flox) owing to the presence of both targeted and deleted *Fh1* alleles.

not possible for technical reasons in the renal cysts of our mice, our data provide further support for the model in which HIF1α stabilization in HLRCC (and HPGL) tumors occurs via inhibition of PHDs by fumarate and/or succinate accumulation (Isaacs et al., 2005; Pollard et al., 2005b; Selak et al., 2005). It remains possible that inhibition of other dioxygenases, such as procollagen prolyl hydroxylases, contributes to tumorigenesis in HLRCC.

Our data suggest that pseudohypoxic drive resulting from *FH* inactivation differs from that caused by *VHL* inactivation. In our mice and HLRCC cases, nuclear expression of HIF1α was greater than that of HIF2α, even though increased HIF2α in many human tumors is associated with enhanced growth and progression (Raval et al., 2005; Xia et al., 2002; Yoshimura et al., 2004). In *Vhl* knockout mice, Hif2α is overexpressed in liver tumors, but in renal cysts (Rankin et al., 2005; Rankin et al., 2006), Hif2α expression has not been detected, nor has Hif1α expression been described. Interestingly, genetic evidence suggests that Hif1α overexpression is not obligatory for renal cyst development in *Vhl* mutant mice, since cysts can form on a

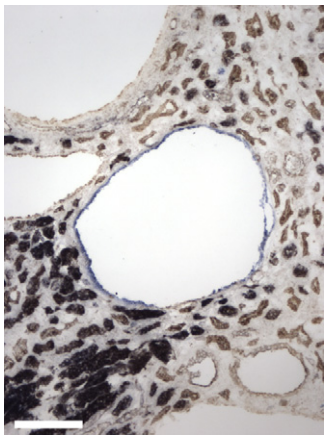

Figure 5. Enzyme Cytochemistry for Cytochrome *c* Oxidase Subunit 1

Enzyme cytochemistry for cytochrome *c* oxidase subunit 1 (A–C) shows absence of expression in central cyst (blue) and expression (brown) in surrounding cysts and normal kidney from an *Fh1*$^{-/-}$ knockout animal. Scale bar, 250 μm for all panels.

Hif1α$^{-/-}$ background. CCRCCs in VHL patients express CAIX strongly (Kivela et al., 2005; Wykoff et al., 2000), and CAIX immunostaining has been used for the identification of early, premalignant renal lesions in VHL disease (Mandriota et al., 2002). Our murine renal cysts and HLRCC tumors, however, revealed very low CAIX expression and no correlation with expression of HIF1α or HIF2α. *VHL* and *FH* inactivation may therefore have differing effects on HIF stabilization and the expression of downstream target genes, perhaps helping to explain the different tissue specificity and tumor spectrum in VHL disease and HLRCC.

The genetic pathway of renal carcinogenesis in HLRCC involves germline inactivation of one *FH* allele and somatic inactivation of the other; there is very little evidence to show that somatic inactivation of both *FH* alleles occurs in sporadic RCCs. We have shown that inactivation of *Fh1* in the kidney causes activation of the hypoxia pathway and modestly increased cellular proliferation that results in numerous, often macroscopic cysts. This phenotype resembles that found in some *Vhl* mutant mice. The lesions in our mice were probably derived from the collecting ducts and thick ascending limb of the loop of Henle, the former corresponding to the probable site of origin of at least some of the cancers in HLRCC. The finding of frequent nuclear HIF overexpression in the cysts of our *Fh1* knockout animals strongly suggests that FH deficiency is a direct cause of the HIF stabilization found in HLRCC tumors. This contention is further supported by the in vitro Cre-mediated inactivation of *Fh1* and subsequent overexpression of Hif1α in our murine *Fh1*$^{fl/-}$ ES cells. It is also plausible, at least in some cases, that a simple cyst → complex cyst/dysplastic cyst → carcinoma exists for HLRCC, as it probably does for VHL disease, with *FH* inactivation as the initiating event in this pathway. While other (epi)genetic events are almost certainly required

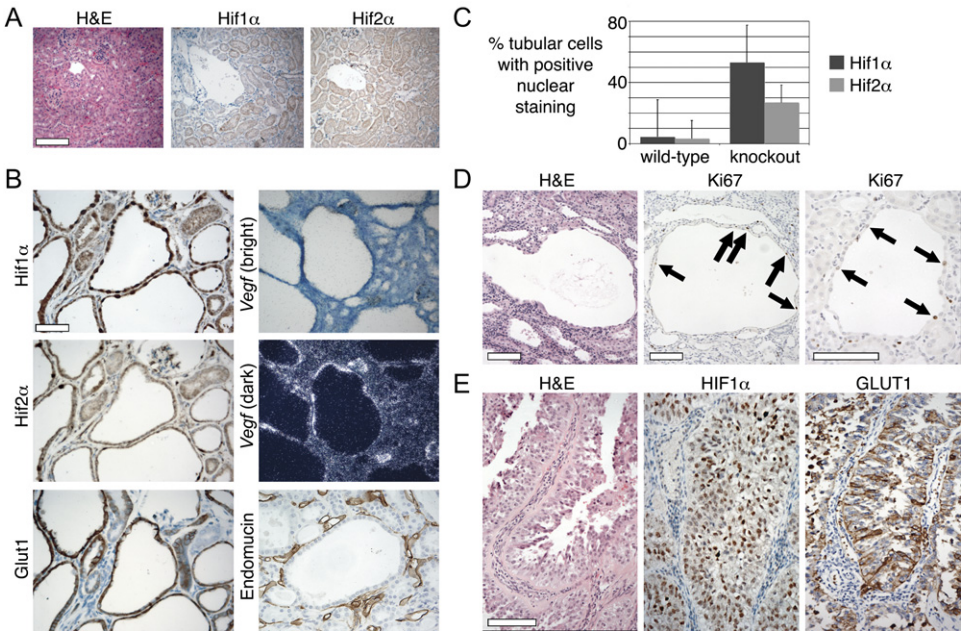

Figure 6. Analysis of Proliferation and Hypoxia-Related Genes in Fh1 Null Renal Cysts and Human Type II Papillary Carcinomas

(A) *Fh1* wild-type kidney shows weak cytoplasmic staining of Hif1α and Hif2α, and absence of nuclear positivity. Scale bar, 250 μm for all panels.

(B) *Fh1* knockout renal cysts show strong nuclear expression of Hif1α in the epithelial layer. Hif2α nuclear staining occurs at a lower frequency than that of Hif1α in cyst epithelium. The protein product of the Hif1-target gene Glut1 is expressed in the epithelial layer, as is *Vegf* mRNA (β-actin control not shown). High vascularity around the lesion is indicated by the endomucin immunostaining. Scale bar, 125 μm for all panels.

(C) The proportions of cyst cells expressing nuclear Hif1α and Hif2α in ten random high-power fields from kidneys derived from each of three control and four knockout mice are shown. The differences between the knockouts and controls were highly statistically significant ($p < 0.0001$ for both Hif1α and Hif2α, Mann-Whitney test). y error bars indicate ± SEM.

(D) A representative renal cyst from an *Fh1* knockout animal shows cells (arrows) with Ki67 immunostaining. Wild-type kidney (not shown) has very little Ki67 expression. Scale bar, 250 μm for all panels.

(E) Human HLRCC type II papillary renal carcinoma shows strong nuclear expression of HIF1α and overexpression of GLUT1. Scale bar, 250 μm for all panels.

for renal cancer in HLRCC, our mouse model may provide a useful model for testing potential therapies for RCC.

EXPERIMENTAL PROCEDURES

Generation and Husbandry of Mice

Following generation of the targeting construct, linearization, and electroporation into 129Sv/J ES cells, stable integrants were selected in 0.2 $mgml^{-1}$ Geneticin G418 medium. Homologous recombinants were identified initially by PCR and subsequently by Southern blot analysis. Targeted ES cells were injected into C57/BL6 blastocysts. The Cancer Research UK Transgenic and Ethics committees approved all procedures involving live animals, and experiments were undertaken in accordance with the Home Office guidelines and licensing regulations (project license number: 70/6018).

DNA Extraction

DNA extraction from ES cells and tail clippings was carried out after overnight digestion at 55°C in extraction buffer (100 mM EDTA [pH 8.0], 50 mM TRIS-HCl [pH 8.0], 100 mM NaCl, 1% SDS [w/v], and 1.0 $mgml^{-1}$ proteinase K). DNA was precipitated by adding isopropanol, washed twice in 70% ethanol (v/v), and resuspended in TE (pH 8.0).

Mouse and ES Cell Genotyping

ES cell clones were screened for 5′ and 3′ site-specific genomic integration of the targeting construct using a PCR-based assay and LA-Taq (Takara). PCR genotypes to assay Flp- and Cre-mediated recombination, and genotyping of eFlp and Cre expression mice were carried out using standard conditions. For the genotyping of *Fh1* to distinguish between wild-type, null, and floxed alleles, a common forward primer (5′-GCTCAGTCACCCATCCAAAT-3′) and differential reverse primers (5′-ACCCTGCTAGGTGTCACCAC-3′ and 5′-CCTGGCACTGCAGACT ACAA-3′) were used. Further details of genotyping are available from the authors on request.

Southern Blotting

Southern blotting of DNA from ES cell clones and mice was performed using standard procedures. In brief, 11 μg of DNA was digested with XcmI, and the DNA was electrophoresed through a 1% agarose gel for 16 hr at 50 V. The gel was depurinated, denatured, and neutralized, and DNA was transferred overnight to Hybond N+ nitocellulose membrane (Amersham). The membrane was UV crosslinked. PCR was used to generate two probes, one of 498 bp with homology to exon 5 of the *Fh1* gene and another of 350 bp derived from the neomycin cassette of the targeting vector. The probes were labeled with α^{32}-dCTP and denatured, before being hybridized to the membrane overnight at 65°C in a rotating oven. The membrane was washed, exposed to film (Kodak) overnight at −80°C, developed, and quantitated by signal intensity of specific-sized bands.

Immunohistochemistry

Processing of tissue and immunochemistry was performed using standard methods. In brief, all mouse tissues were fixed in neutral-buffered 10% formalin for 24 hr. Antigen retrieval was performed by microwaving in citrate buffer (pH 6.0) for 10–15 min. Primary antibodies: laminin

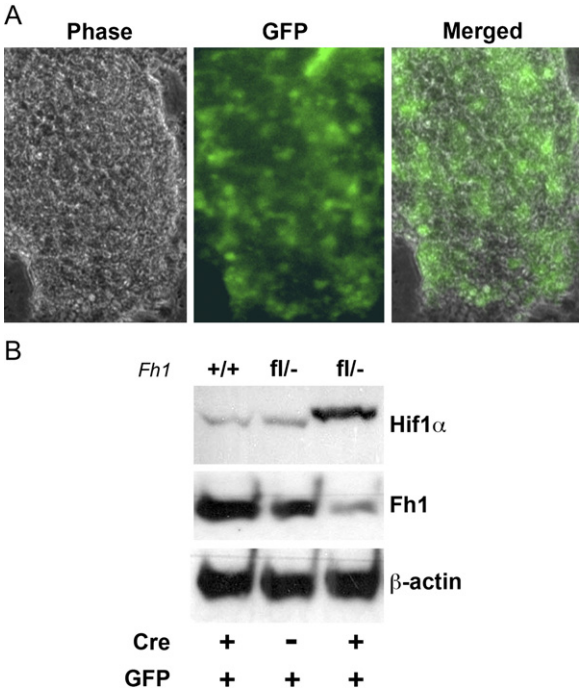

Figure 7. Fh1 Knockout in Embryonic Stem Cells Causes Upregulation of Hif1α

(A) Visualization of eGFP in ES cells 48 hr posttransfection with pCre-IREShrGFPII using low-power light microscopy.

(B) Western blotting of FACS-sorted ES cells showing HIf1α, Fh1, and β-actin (loading control). Note that low levels of endogenous Hif1α are present in wild-type cells and in $Fh1^{fl/-}$ cells in the absence of Cre. Cre-mediated removal of the targeted *Fh1* allele was confirmed by genomic PCR (not shown) and consistently resulted in very little Fh1 protein and greatly increased (>5-fold) Hif1α.

(Abcam), Oct4 (CeMines), THP (Biogenesis), aquaporin2 (R&D Systems), endomucin (kind gift from Dr Vestweber, Germany), and Ki67 (Dako). Immunohistochemistry for Hif1α, Hif2α (Epas1), Glut1, and Caix was carried out as previously described (Talks et al., 2000), and the apoptosis was assessed using the DeadEnd colorimetric TUNEL kit (Promega). Expression was assessed by three independent observers (P.J.P., M.D., and D.S.) as follows. For aquaporin2, Caix, Glut1, and Thp, cysts were scored as showing positive or negative expression. For Ki67 and TUNEL, positive nuclei were counted per high-power field (×400) in both wild-type and knockout kidneys, and the percentage positivity was calculated per cyst. For Hif1α and Hif2α, each section was initially assessed for nuclear expression. The numbers and proportions of positive nuclei (Hif1α and Hif2α) per cyst were calculated in whole kidney sections from eight animals (four knockouts, four control). For the five HLRCC type II papillary RCC, total and positive nuclei were counted in ten high-power fields (×400), and the percentage of positive nuclei was determined for each HIF isoform. Unpaired normal kidney and stromal cells within the tumor sections were used as negative controls.

In Situ Hybridization

In situ hybridization was carried out using 4 μm serial sections from the same formalin-fixed, paraffin-embedded specimens as used for immunohistochemistry. The murine *Fh1* probe (230 bp) was PCR amplified from cDNA using the primers 5′- CGGGGTACCTGAAGCG AGCTGCTGCTGAAGTA-3′ and 5′-CCGGAATTCCACAGGCTTCTT GCTGCCAAGTT-3′ (restriction sites underlined), cloned into pGEM-3Z (Promega) using EcoRI and KpnI, and linearized with BamHI. Antisense RNA was generated by T7 polymerase. For hybridization control, a β-actin probe (~414 bases) was generated from DraI-linearized pSP73 (Promega) containing clone hbA-10. *Vegf* and *Tgfa* ISH have previously been described (Goldenring et al., 1996; Huminiecki et al., 2001). α^{35}S-UTP labeling, hybridization, and processing for all probes were performed as previously described (Poulsom et al., 1998). Signal intensity was scored by two independent observers (P.J.P. and R.P.) as absent, weak, moderate, or strong for all sections for which β-actin signal passed quality control threshold.

Laser-Capture Microdissection

Kidney sections (5 μm) were stained with methylene green, and renal cortex and cysts were isolated using LCM (Palm@Robo V2.2, P.A.L.M Microlaser Technologies) at ×400 magnification and illumination (Carl Zeiss, HAL 100). DNA was extracted using the PicoPure kit (Arcturus) using the manufacturer's protocol. DNA was PCR amplified as described in the mouse genotyping methods.

Enzyme Histochemistry

Frozen sections were cut at a thickness of 12 μm. Sequential cytochrome *c* oxidase and succinate dehydrogenase (used to highlight any deficiencies in cytochrome *c* oxidase) histochemistry was performed as previously described (Taylor et al., 2003). We found no evidence that Fh1 deficiency had a detrimental effect on this assay, as the great majority of $Fh1^{-/-}$ cysts showed normal expression of cytochrome *c* oxidase, as expected. Briefly, air-dried sections were incubated with a cytochrome *c* oxidase medium containing 100 mM cytochrome *c*, 20 mg/ml catalase, and 4 mM diaminobenzidine tetrahydrochloride in 0.2 M phosphate buffer (pH 7.0), all sourced from Sigma Aldrich (Poole, UK) for a maximum of 2 min at 37°C (or until no increase in staining intensity was observed). Sections were then washed in phosphate-buffered saline buffer (pH 7.4) (PBS) three times for 5 min and then incubated in SDH medium (130 mM sodium succinate, 200 mM phenazine methosulphate, 1 mM sodium azide, and 1.5 mM nitroblue tetrazolium in 0.2 M phosphate buffer [pH 7.0]).

ES Cell Culture and Transfection

$Fh1^{fl/-}$ ES cells were derived from blastocysts (E3.5) taken from matings between $Fh1^{fl/fl}$ and $Fh1^{fl/-}$ mice using standard procedures (Nagy et al., 2003). Cells were maintained in culture under standard conditions (Nagy et al., 2003). For transfections, ES cells were trypsinized and then plated on gelatin-coated tissue culture plates 24 hr prior to transfection. The cDNA coding sequence for Cre recombinase was cloned into pIREShrGFPII (Stratagene, CA, USA), in which GFP is expressed using an IRES, using standard procedures. Cells were transfected with 4 μg of pCre-IREShrGFPII or pIREShrGFPII with 1.5 μg of Lipofectamine 2000 (Gibco-BRL, MD, USA). The transfected cells were harvested after 48 hr and viewed under a low-light microscope (Nikon) to assay fluorescence. Cells were trypsinized, centrifuged, suspended in chilled PBS, and subjected to fluorescence-activated cell sorting (FACS) analysis on the basis of GFP expression using a MOFLOW flow cytometer (Dakocytomation, CO, USA).

Western Blotting

FACS-sorted cells were pelleted and washed twice in PBS, and protein was extracted using standard methods as previously described (Pollard et al., 2005b). Fifty micrograms of total protein was resolved through Tris-Acetate gels at constant current (30 mA) and transferred to PDVF membrane using the NuPage/iBlot system (Invitrogen) following the manufacturer's protocol. Antibodies (anti-Hif1α [Abcam] 1/1000, anti-β-actin [Sigma] 1/1000, and anti-fumarase [Nordic] 1/400) were applied in 3% dried milk, constituted in PBS, and hybridized overnight at 4°C. Secondary antibody (Dako) was applied 1/5000 for 45 min at room temperature. Proteins were detected using the ECL technique (Amersham Pharmacia, UK) and visualized by scanning and densitometry, comparing the Hif1α and Fh1 levels to the β-actin control.

Statistical Analysis

Expression levels of genes and proteins were compared in test and control animals or cells using the Mann-Whitney test.

ACKNOWLEDGMENTS

We gratefully acknowledge the animal technicians at Clare Hall Laboratories for the breeding and husbandry of the mice, Gavin Kelly in the Biostatistics and Bioinformatics Department at Cancer Research UK for advice on statistical analysis, Rob Nicolas and Andrew Rowan for technical advice, and Dr. D. Vestweber for providing the endomucin antibody.

Received: September 9, 2006
Revised: December 14, 2006
Accepted: February 6, 2007
Published: April 9, 2007

REFERENCES

Alam, N.A., Rowan, A.J., Wortham, N.C., Pollard, P.J., Mitchell, M., Tyrer, J.P., Barclay, E., Calonje, E., Manek, S., Adams, S.J., et al. (2003). Genetic and functional analyses of FH mutations in multiple cutaneous and uterine leiomyomatosis, hereditary leiomyomatosis and renal cancer, and fumarate hydratase deficiency. Hum. Mol. Genet. *12*, 1241–1252.

Alam, N.A., Olpin, S., and Leigh, I.M. (2005). Fumarate hydratase mutations and predisposition to cutaneous leiomyomas, uterine leiomyomas and renal cancer. Br. J. Dermatol. *153*, 11–17.

Baysal, B.E., Willett-Brozick, J.E., Lawrence, E.C., Drovdlic, C.M., Savul, S.A., McLeod, D.R., Yee, H.A., Brackmann, D.E., Slattery, W.H., 3rd, Myers, E.N., et al. (2002). Prevalence of SDHB, SDHC, and SDHD germline mutations in clinic patients with head and neck paragangliomas. J. Med. Genet. *39*, 178–183.

Binienda, Z.K., Sadovova, N.V., Rountree, R.L., Scallet, A.C., and Ali, S.F. (2001). Effect of L-carnitine pretreatment on 3-nitropropionic acid-induced inhibition of rat brain succinate dehydrogenase activity. Ann. N Y Acad. Sci. *939*, 359–365.

Boado, R.J., and Pardridge, W.M. (2002). Glucose deprivation and hypoxia increase the expression of the GLUT1 glucose transporter via a specific mRNA cis-acting regulatory element. J. Neurochem. *80*, 552–554.

Carmeliet, P., Dor, Y., Herbert, J.M., Fukumura, D., Brusselmans, K., Dewerchin, M., Neeman, M., Bono, F., Abramovitch, R., Maxwell, P., et al. (1998). Role of HIF-1alpha in hypoxia-mediated apoptosis, cell proliferation and tumour angiogenesis. Nature *394*, 485–490.

Gimenez-Roqueplo, A.P., Favier, J., Rustin, P., Mourad, J.J., Plouin, P.F., Corvol, P., Rotig, A., and Jeunemaitre, X. (2001). The R22X mutation of the SDHD gene in hereditary paraganglioma abolishes the enzymatic activity of complex II in the mitochondrial respiratory chain and activates the hypoxia pathway. Am. J. Hum. Genet. *69*, 1186–1197.

Gimenez-Roqueplo, A.P., Favier, J., Rustin, P., Rieubland, C., Kerlan, V., Plouin, P.F., Rotig, A., and Jeunemaitre, X. (2002). Functional consequences of a SDHB gene mutation in an apparently sporadic pheochromocytoma. J. Clin. Endocrinol. Metab. *87*, 4771–4774.

Goldenring, J.R., Poulsom, R., Ray, G.S., Wright, N., Meise, K.S., and Coffey, R.J., Jr. (1996). Expression of trefoil peptides in the gastric mucosa of transgenic mice overexpressing transforming growth factor-alpha. Growth Factors *13*, 111–119.

Greaves, L.C., Preston, S.L., Tadrous, P.J., Taylor, R.W., Barron, M.J., Oukrif, D., Leedham, S.J., Deheragoda, M., Sasieni, P., Novelli, M.R., et al. (2006). Mitochondrial DNA mutations are established in human colonic stem cells, and mutated clones expand by crypt fission. Proc. Natl. Acad. Sci. USA *103*, 714–719.

Huminiecki, L., Chan, H.Y., Lui, S., Poulsom, R., Stamp, G., Harris, A.L., and Bicknell, R. (2001). Vascular endothelial growth factor transgenic mice exhibit reduced male fertility and placental rejection. Mol. Hum. Reprod. *7*, 255–264.

Iliopoulos, O., and Kaelin, W.G., Jr. (1997). The molecular basis of von Hippel-Lindau disease. Mol. Med. *3*, 289–293.

Isaacs, J.S., Jung, Y.J., Mole, D.R., Lee, S., Torres-Cabala, C., Chung, Y.L., Merino, M., Trepel, J., Zbar, B., Toro, J., et al. (2005). HIF overexpression correlates with biallelic loss of fumarate hydratase in renal cancer: Novel role of fumarate in regulation of HIF stability. Cancer Cell *8*, 143–153.

Ivan, M., Kondo, K., Yang, H., Kim, W., Valiando, J., Ohh, M., Salic, A., Asara, J.M., Lane, W.S., and Kaelin, W.G., Jr. (2001). HIFalpha targeted for VHL-mediated destruction by proline hydroxylation: Implications for O2 sensing. Science *292*, 464–468.

Jaakkola, P., Mole, D.R., Tian, Y.M., Wilson, M.I., Gielbert, J., Gaskell, S.J., Kriegsheim, A., Hebestreit, H.F., Mukherji, M., Schofield, C.J., et al. (2001). Targeting of HIF-alpha to the von Hippel-Lindau ubiquitylation complex by O2-regulated prolyl hydroxylation. Science *292*, 468–472.

Kiuru, M., and Launonen, V. (2004). Hereditary leiomyomatosis and renal cell cancer (HLRCC). Curr. Mol. Med. *4*, 869–875.

Kiuru, M., Launonen, V., Hietala, M., Aittomaki, K., Vierimaa, O., Salovaara, R., Arola, J., Pukkala, E., Sistonen, P., Herva, R., and Aaltonen, L.A. (2001). Familial cutaneous leiomyomatosis is a two-hit condition associated with renal cell cancer of characteristic histopathology. Am. J. Pathol. *159*, 825–829.

Kivela, A.J., Parkkila, S., Saarnio, J., Karttunen, T.J., Kivela, J., Parkkila, A.K., Bartosova, M., Mucha, V., Novak, M., Waheed, A., et al. (2005). Expression of von Hippel-Lindau tumor suppressor and tumor-associated carbonic anhydrases IX and XII in normal and neoplastic colorectal mucosa. World J. Gastroenterol. *11*, 2616–2625.

Lehtonen, H.J., Kiuru, M., Ylisaukko-Oja, S.K., Salovaara, R., Herva, R., Koivisto, P.A., Vierimaa, O., Aittomaki, K., Pukkala, E., Launonen, V., and Aaltonen, L.A. (2005). Increased risk of cancer in patients with fumarate hydratase germline mutation. J. Med. Genet. *43*, 523–526.

Levy, A.P., Levy, N.S., and Goldberg, M.A. (1996). Hypoxia-inducible protein binding to vascular endothelial growth factor mRNA and its modulation by the von Hippel-Lindau protein. J. Biol. Chem. *271*, 25492–25497.

Lisztwan, J., Imbert, G., Wirbelauer, C., Gstaiger, M., and Krek, W. (1999). The von Hippel-Lindau tumor suppressor protein is a component of an E3 ubiquitin-protein ligase activity. Genes Dev. *13*, 1822–1833.

Maher, E.R., and Kaelin, W.G., Jr. (1997). von Hippel-Lindau disease. Medicine (Baltimore) *76*, 381–391.

Mandriota, S.J., Turner, K.J., Davies, D.R., Murray, P.G., Morgan, N.V., Sowter, H.M., Wykoff, C.C., Maher, E.R., Harris, A.L., Ratcliffe, P.J., and Maxwell, P.H. (2002). HIF activation identifies early lesions in VHL kidneys: Evidence for site-specific tumor suppressor function in the nephron. Cancer Cell *1*, 459–468.

Masson, N., and Ratcliffe, P.J. (2003). HIF prolyl and asparaginyl hydroxylases in the biological response to intracellular O(2) levels. J. Cell Sci. *116*, 3041–3049.

Maxwell, P.H., Wiesener, M.S., Chang, G.W., Clifford, S.C., Vaux, E.C., Cockman, M.E., Wykoff, C.C., Pugh, C.W., Maher, E.R., and Ratcliffe, P.J. (1999). The tumour suppressor protein VHL targets hypoxia-inducible factors for oxygen-dependent proteolysis. Nature *399*, 271–275.

Nagy, A., Gertsenstein, M., and Bintersten, K.R. (2003). Manipulating the Mouse Embryo: A Laboratory Manual, Third Edition (Cold Spring Harbor, NY: Cold Spring Harbor Laboratory Press).

Pollard, P., Wortham, N., Barclay, E., Alam, A., Elia, G., Manek, S., Poulsom, R., and Tomlinson, I. (2005a). Evidence of increased microvessel density and activation of the hypoxia pathway in tumours from the hereditary leiomyomatosis and renal cell cancer syndrome. J. Pathol. *205*, 41–49.

Pollard, P.J., Briere, J.J., Alam, N.A., Barwell, J., Barclay, E., Wortham, N.C., Hunt, T., Mitchell, M., Olpin, S., Moat, S.J., et al. (2005b). Accumulation of Krebs cycle intermediates and over-expression of HIF1 {alpha} in tumours which result from germline FH and SDH mutations. Hum. Mol. Genet. *14*, 2231–2239.

Poulsom, R., Longcroft, J.M., Jeffery, R.E., Rogers, L.A., and Steel, J.H. (1998). A robust method for isotopic riboprobe in situ hybridisation to localise mRNAs in routine pathology specimens. Eur. J. Histochem. *42*, 121–132.

Pugh, C.W., and Ratcliffe, P.J. (2003). Regulation of angiogenesis by hypoxia: Role of the HIF system. Nat. Med. *9*, 677–684.

Rankin, E.B., Higgins, D.F., Walisser, J.A., Johnson, R.S., Bradfield, C.A., and Haase, V.H. (2005). Inactivation of the arylhydrocarbon receptor nuclear translocator (Arnt) suppresses von Hippel-Lindau disease-associated vascular tumors in mice. Mol. Cell. Biol. *25*, 3163–3172.

Rankin, E.B., Tomaszewski, J.E., and Haase, V.H. (2006). Renal cyst development in mice with conditional inactivation of the von Hippel-Lindau tumor suppressor. Cancer Res. *66*, 2576–2583.

Raval, R.R., Lau, K.W., Tran, M.G., Sowter, H.M., Mandriota, S.J., Li, J.L., Pugh, C.W., Maxwell, P.H., Harris, A.L., and Ratcliffe, P.J. (2005). Contrasting properties of hypoxia-inducible factor 1 (HIF-1) and HIF-2 in von Hippel-Lindau-associated renal cell carcinoma. Mol. Cell. Biol. *25*, 5675–5686.

Schofield, C.J., and Ratcliffe, P.J. (2004). Oxygen sensing by HIF hydroxylases. Nat. Rev. Mol. Cell Biol. *5*, 343–354.

Selak, M.A., Armour, S.M., MacKenzie, E.D., Boulahbel, H., Watson, D.G., Mansfield, K.D., Pan, Y., Simon, M.C., Thompson, C.B., and Gottlieb, E. (2005). Succinate links TCA cycle dysfunction to oncogenesis by inhibiting HIF-alpha prolyl hydroxylase. Cancer Cell *7*, 77–85.

Shao, X., Johnson, J.E., Richardson, J.A., Hiesberger, T., and Igarashi, P. (2002a). A minimal Ksp-cadherin promoter linked to a green fluorescent protein reporter gene exhibits tissue-specific expression in the developing kidney and genitourinary tract. J. Am. Soc. Nephrol. *13*, 1824–1836.

Shao, X., Somlo, S., and Igarashi, P. (2002b). Epithelial-specific Cre/lox recombination in the developing kidney and genitourinary tract. J. Am. Soc. Nephrol. *13*, 1837–1846.

Talks, K.L., Turley, H., Gatter, K.C., Maxwell, P.H., Pugh, C.W., Ratcliffe, P.J., and Harris, A.L. (2000). The expression and distribution of the hypoxia-inducible factors HIF-1alpha and HIF-2alpha in normal human tissues, cancers, and tumor-associated macrophages. Am. J. Pathol. *157*, 411–421.

Taylor, R.W., Barron, M.J., Borthwick, G.M., Gospel, A., Chinnery, P.F., Samuels, D.C., Taylor, G.A., Plusa, S.M., Needham, S.J., Greaves, L.C., et al. (2003). Mitochondrial DNA mutations in human colonic crypt stem cells. J. Clin. Invest. *112*, 1351–1360.

Tomlinson, I.P., Alam, N.A., Rowan, A.J., Barclay, E., Jaeger, E.E., Kelsell, D., Leigh, I., Gorman, P., Lamlum, H., Rahman, S., et al. (2002). Germline mutations in FH predispose to dominantly inherited uterine fibroids, skin leiomyomata and papillary renal cell cancer. Nat. Genet. *30*, 406–410.

Toro, J.R., Nickerson, M.L., Wei, M.H., Warren, M.B., Glenn, G.M., Turner, M.L., Stewart, L., Duray, P., Tourre, O., Sharma, N., et al. (2003). Mutations in the fumarate hydratase gene cause hereditary leiomyomatosis and renal cell cancer in families in North America. Am. J. Hum. Genet. *73*, 95–106.

Wang, G.L., Jiang, B.H., Rue, E.A., and Semenza, G.L. (1995). Hypoxia-inducible factor 1 is a basic-helix-loop-helix-PAS heterodimer regulated by cellular O2 tension. Proc. Natl. Acad. Sci. USA *92*, 5510–5514.

Wykoff, C.C., Beasley, N.J., Watson, P.H., Turner, K.J., Pastorek, J., Sibtain, A., Wilson, G.D., Turley, H., Talks, K.L., Maxwell, P.H., et al. (2000). Hypoxia-inducible expression of tumor-associated carbonic anhydrases. Cancer Res. *60*, 7075–7083.

Xia, G., Kageyama, Y., Hayashi, T., Hyochi, N., Kawakami, S., and Kihara, K. (2002). Positive expression of HIF-2alpha/EPAS1 in invasive bladder cancer. Urology *59*, 774–778.

Yoshimura, H., Dhar, D.K., Kohno, H., Kubota, H., Fujii, T., Ueda, S., Kinugasa, S., Tachibana, M., and Nagasue, N. (2004). Prognostic impact of hypoxia-inducible factors 1alpha and 2alpha in colorectal cancer patients: correlation with tumor angiogenesis and cyclooxygenase-2 expression. Clin. Cancer Res. *10*, 8554–8560.

Zeevalk, G.D., Derr-Yellin, E., and Nicklas, W.J. (1995). Relative vulnerability of dopamine and GABA neurons in mesencephalic culture to inhibition of succinate dehydrogenase by malonate and 3-nitropropionic acid and protection by NMDA receptor blockade. J. Pharmacol. Exp. Ther. *275*, 1124–1130.